Flows around Confined Bubbles and Their Importance in Triggering Pinch-Off

Volkert van Steijn,[1] Chris R. Kleijn,[1] and Michiel T. Kreutzer[2,*]

[1]*Multiscale Physics, Delft University of Technology, Prins Berhardlaan 6, 2628 BW Delft, The Netherlands*
[2]*Department of Chemical Engineering, Delft University of Technology, Julianalaan 136, 2628 BL Delft, The Netherlands*

(Received 8 April 2009; published 19 November 2009)

We describe the breakup of a confined gas thread in a cross-flowing stream of liquid at capillary numbers $\mathrm{Ca} < 10^{-2}$. The breakup is initiated, not by a Plateau-Rayleigh instability, but by liquid that flows from the tip of the thread to the neck where pinch-off occurs. This flow, faster than previously estimated, is driven by different curvatures at the tip and neck and runs through large gaps between thread and channel walls. Understanding how these curvatures evolve during bubble formation leads to accurate predictions of the moment of pinch-off.

DOI: 10.1103/PhysRevLett.103.214501 PACS numbers: 47.55.D−, 47.20.Ma, 68.03.Cd, 82.70.−y

The formation of bubbles and droplets from a continuous thread has been a celebrated problem in fluid mechanics since the seminal works of Rayleigh and Plateau [1] that explain the kitchen-sink experiment of a dripping faucet as a capillary instability, driven thermodynamically by the minimization of surface energy, where the size of the drop is determined by the wavelength of the fastest growing disturbance. Recently, microfluidic devices that coflow immiscible fluids to generate microbubbles and microdroplets have been developed in geometries such as T junctions [2,3] and flow-focusing devices [4]. In such geometries where the thread touches the walls, the monodispersity of bubbles is superior to that of those generated in unconfined flows. This is attributed to an absence of nonlinear dynamics in the breakup [5]. These monodisperse microbubbles and microdroplets of picoliter and nanoliter volume are indispensable in applications such as ''digital'' microfluidics, high-throughput chemical synthesis, medical screening, and contrast agents [6].

Confinement is most important at low values of the capillary number ($\mathrm{Ca} = \eta U/\gamma$, with velocity of the liquid U, surface tension γ, and viscosity η). When $\mathrm{Ca} < 10^{-2}$, a thread can grow to occupy most of the channel cross section (as shown in Fig. 1), instead of being sheared off by the liquid early in its growth and remaining small, which is what happens at high Ca [7]. Experiments show that a growing thread of gas is squeezed initially such that the radius of the neck of the thread decreases linearly in time. Then, at a geometry-dependent moment, the neck of the thread collapses at an accelerated tempo. An important practical question is how and when the *pinch-off* occurs, because that determines the size of the bubbles.

In this Letter, we resolve a debate on this rapid thread collapse. On a fundamental level, the physical mechanism that triggers it is still unclear. One view is that the neck, as soon as it detaches from the wall, can be approximated as a detached thread. Such detached threads are always unstable in round and rectangular channels [8]. Dollet *et al.* [9] interpreted pinch-off using a linear stability analysis, based on their experimental finding that the start of the rapid collapse of the neck coincides with the ''lift-off'' of the shrinking thread from the wall. Another view, argued by Garstecki *et al.* [10], is that the bubble remains stable as the neck starts to collapse, evolving near the neck in quasistatic equilibria of minimal surface energy, in contrast with the nonequilibrium Plateau-Rayleigh instability. In their analysis, the rapid constriction gives a false impression of a small disturbance that grows exponentially, and the constriction occurs solely because the coflowing liquid cannot bypass the growing bubble, leaving it no option other than to squeeze the neck. To support their argument, they have numerically calculated equilibrium shapes of the neck with thread volume as a free parameter, noting that the neck rapidly collapses below a certain volume. Interestingly, this calculation also predicted a rapid constriction as soon as the thread releases from the wall.

As the experimental evidence in flow-focusing devices seems to support different theories, we use an alternative geometry, depicted in Fig. 1. We demonstrate here that the thread remains stable as it detaches from the wall. Rather, the collapse of the thread is triggered by a sudden flow of liquid to the neck from the tip of the thread, which has to date been ignored for confined bubble formation.

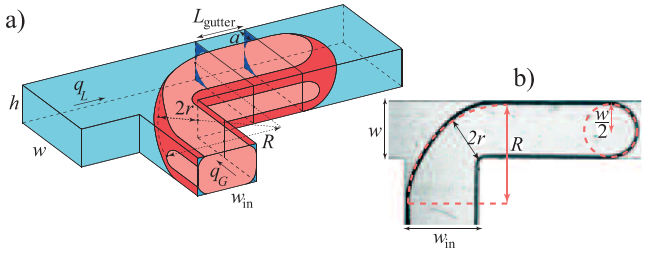

FIG. 1 (color online). (a) Sketch of a bubble growing at a planar T junction with height h and widths w and w_{in}. The bubble does not fully occupy the channels but leaves gutters with curvature a^{-1} and length L_{gutter}. (b) Micrograph showing the radii of curvature r (out-of-plane) and R (in-plane). We measured $2r$ as the shortest distance from the interface to the lower-right corner of the junction and R by fitting a quarter of a circle to the interface, as in [20].

Crucially, channels that confine bubble-forming threads are rectangular (a few noted exceptions, e.g., Ref. [11], use axisymmetric devices), such that *gutters* of liquid exist in the corners [12]. These gutters exist with or without flow, and the usual assumption at small Ca is that their shape is hardly affected by flow. Flow in these gutters is driven by the difference in pressure over the growing thread, which to leading order depends on the difference in curvature κ via the Laplace-Young equation $p = \gamma\kappa$. Velocities in the gutters, relative to that of the growing thread itself, depend strongly on the shape of the gutters and channels, as described by Wong [13]. As we show below, we observe velocities that are comparable to those of the thread at Ca $\sim 10^{-3}$. At even lower Ca, Ca $\ll 10^{-4}$, another regime appears where the dominant velocity will actually be in the gutters, making it hard to move the bubble [14].

We created microchannel networks in polydimethylsiloxane on glass slides, using standard soft lithography methods, featuring T-junction geometries of different heights h, liquid channel widths w, and gas channel widths w_{in}. Ethanol (99.5 v/v%) was used as the liquid without surfactants, with viscosity $\eta = 1.2$ mPa s, surface tension $\gamma = 0.02$ N/m, and equilibrium contact angle $\theta_e < 10°$. The liquid feed rate q_L was controlled using a syringe pump in the range 1–32 μL/min. A steady flow of air q_G, 1–32 μL/min, was fed into the gas channel through a 2-m-long capillary of 100 μm internal diameter. The shape of the growing bubble was recorded with a high-speed camera at 10 000 frames per second. In one geometry, the velocities in a plane parallel to the top wall, at $0.1h$ from the top wall, were recorded with microparticle image velocimetry, as described in [15].

The formation of bubbles in a T junction follows two stages [3]: initially, the gas enters into the main channel until it meets the wall opposite of the gas feed channel. This filling stage is followed by a squeezing stage [interfaces a–f in the inset of Fig. 2(a)] in which the interface in the junction is squeezed by the incoming liquid while the thread grows into the main channel. We recorded the time evolution of principal radii of curvature r and R behind the forming bubble, as indicated in Fig. 1. At first, the neck shrinks at an almost constant speed dr/dt. We determine graphically from $r(t)$ a critical value r_{crit} (interface g) that marks the crossover from this linear squeezing to a rapid collapse of the neck (interface h), which we will address shortly. First, we note that the bubble does not completely seal off the channel for the liquid. The solid lines in Fig. 2(a) indicate the interface evolution $(R(t), r(t))$ for the hypothetical case that the liquid pushes the interface without leakage. The interface fits to a toroid, such that $dR/dt = 16q_L/h(4-\pi)(8R + h\pi)$ and $2r - \epsilon = R - [(R-w)^2 + (R - w_{\text{in}})^2]^{1/2}$ for $R > w_{\text{in}}$ and $2r - \epsilon = [w^2 + (R - w_{\text{in}})^2]^{1/2}$ otherwise ($\epsilon \approx 0.1w$ accounts for the rounded corners of the T junction). The dashed line represents the case that 1/10 of the incoming liquid bypasses the bubble, which agrees best with the experiment,

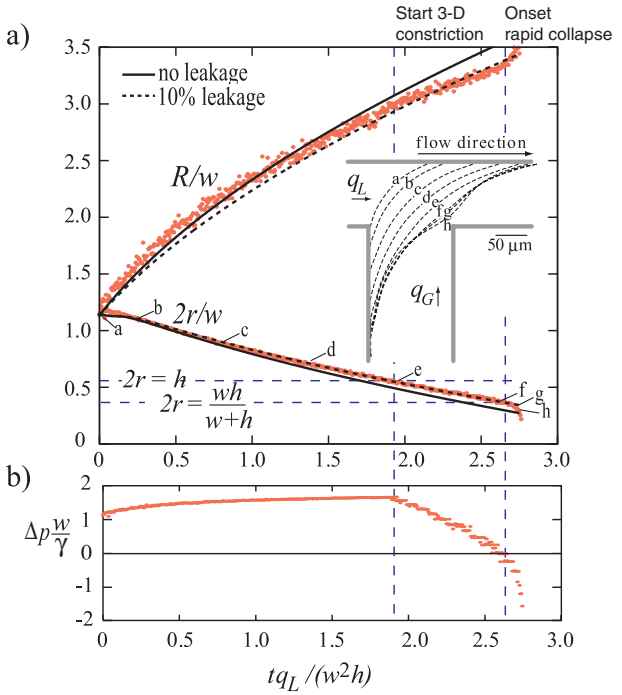

FIG. 2 (color online). (a) Evolution of the radii of curvature r and R. The full line indicates how fast the interface would be squeezed without leakage through the gutters; the dashed line is based on a leakage of 10% of the incoming flow q_L. (b) Evolution of the pressure drop over the gutters, calculated from (a) and Eq. (1), indicating that the collapse coincides with reversal of pressure drop in the gutters. [$(h, w, w_{\text{in}}) = (56, 100, 133)$ μm, $(q_L, q_G) = (2, 17)$ μL, Ca $= 3 \times 10^{-4}$.]

at least in a time-averaged analysis. The leakage is negligible initially and increases until the moment of pinch-off.

Whereas we infer the leakage from Fig. 2(a) indirectly, instantaneous velocity fields in Fig. 3 confirm it. When the thread has just detached from the wall, in Fig. 3(a), the velocity in the gutters is significant and directed downstream. The detachment of the neck is evident from the liquid, rushing into the gap that has opened between the thread and the wall. Then, consider a snapshot during collapse, just before the thread breaks, in Fig. 3(b). The velocity in the gutters has reversed direction, such that liquid flows

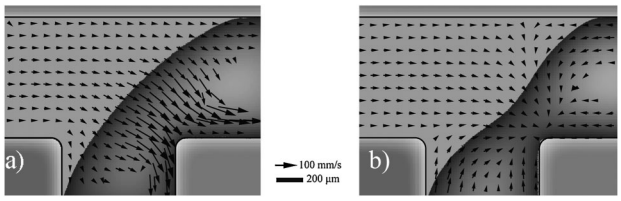

FIG. 3. In-plane velocity at $0.1h$ from the top wall, with a drawing of the neck shape, before and after the start of the rapid collapse. (a) The thread has lifted from the wall, and liquid flows through the gap between the thread and the wall. Flow in the gutters runs towards the tip. (b) The thread has started to collapse. Liquid now runs from the tip to the neck through all four gutters. ($h = w = w_{\text{in}} = 800$ μm, Ca $= 5.7 \times 10^{-4}$.)

back to the neck from the tip. In the following, we show that this reversal can be understood in terms of the pressure profile around the thread. With the pressure in the gas as the reference pressure, the pressure in the liquid at the squeezing interface is given by $p = \gamma[1/R + \min(2/h, 1/r)]$. Similarly for the liquid at the tip, $p = \gamma(2/h + 2/w)$, such that the pressure drop over the gutters is

$$\Delta p = \gamma\left[\frac{2}{h} + \frac{2}{w} - \frac{1}{R} - \min\left(\frac{2}{h}, \frac{1}{r}\right)\right]. \quad (1)$$

Figure 2(b) shows the evolution of this pressure, which increases initially due to the increase of R and then drops as the out-of-plane radius of curvature decreases when the neck detaches from the top and bottom walls. Subsequently, the pressure difference changes sign and the flow in the gutters reverses to drive liquid back to the squeezed neck. It is at this moment of flow reversal that the thread starts to collapse.

Before we analyze when this flow reversal occurs in other devices, we observe here that our results are incompatible with the view that the collapse is initiated by a capillary instability of the gas thread upon *local* detachment from the walls at $2r = h$, which occurs in Fig. 2(a) at $tq_L/(w^2h) \approx 1.9$ without any appreciable change in dr/dt. A thread that touches the channel walls on both sides of a neck is not equivalent, as far as its stability goes, to a thread as thin as the neck that nowhere touches the walls.

We now show that understanding the mechanism permits a prediction of the collapse in different T junctions. Based on Eq. (1), the reversal of flow that triggers the rapid collapse of the thread occurs at $2r_{\mathrm{crit}} = hw/(w + h)$. In deriving this criterion, we neglect the smallest term $1/R$ in the equation, strictly valid because $hw/2R(h + w) \ll 1$ when $h/w \leq 1$ and $R \gtrsim 2w$ at pinch-off. Furthermore, in the final stages (interfaces f-h), the local in-plane curvature at the neck, R', becomes concave and deviates from R as defined in Fig. 1. Yet here, too, $|R'| \gtrsim 2w$ and $hw/2R'(h + w)$ changes sign but, importantly, remains small. With this simplification, the collapse becomes insensitive to the shape of the gas inlet channel. We have repeated the measurements in a range of T-junction geometries ($0.1 < h/w < 1, 0.33 < w_{\mathrm{in}}/w < 3$). Figure 4 shows excellent agreement with this simplest analysis. In shallow devices with $h \ll w$, the term $2/w$ can also be neglected and the criterion simplifies to $2r_{\mathrm{crit}} = h$. In geometries with aspect ratio h/w closer to unity, the term $2/w$ in Eq. (1) cannot be ignored and the collapse happens long after the neck has started to constrict three dimensionally, with $2r = h/2$ in a channel of square cross section. Thus, a solid conclusion can be drawn: the collapse depends only on the moment of flow reversal in the gutters, which in turn can be predicted accurately from the geometry of the bubble generating device.

It is worth emphasizing that the pinch-off is initiated by an additional influx—through gutters around the forming bubble—that depends on the *entire* shape of the interface. In the following, we will demonstrate this from experiments in which the bubble shape far from the neck is varied while keeping the local geometry at the neck unchanged. We created a device, shown in Fig. 5, with a slowly increasing channel width downstream of the T junction. We could now independently vary the curvature at the tip of the thread by playing with the feed rates of the gas and liquid [16]: increasing q_G or decreasing q_L grows the bubble deeper into the channel before it pinches. We recorded the principle radii of curvature at the tip and the squeezed interface as before and measured at the onset of collapse the neck radius r_{crit} and the distance x that the bubble has traveled. We plot these together in Fig. 5. Now a bubble-length dependent radius of curvature at the tip $w_{\mathrm{tip}}(x)$ appears in the collapse criterion $2r(x) = hw_{\mathrm{tip}}(x)/[w_{\mathrm{tip}}(x) + h]$, plotted in Fig. 5 using $w_{\mathrm{tip}} = w + 2x\tan\phi$. A reduction of bubble curvature far from the neck triggers an earlier flow reversal that leads to an earlier pinch-off. This also teaches that flow reversal causes pinch-off, not

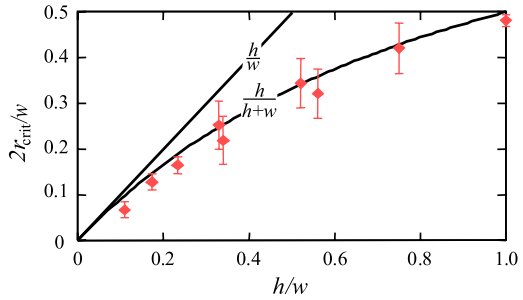

FIG. 4 (color online). Onset of the rapid collapse $2r_{\mathrm{crit}}/w$ as a function of the ratio h/w. The theoretical prediction $2r_{\mathrm{crit}}/w = h/(w + h)$ describes when the flow reverses in the gutters. The line $2r_{\mathrm{crit}}/w = h/w$ describes when the thread detaches from the wall. The error bars reflect the uncertainty in determining the sudden change of dr/dt in graphs such as Fig. 2(a).

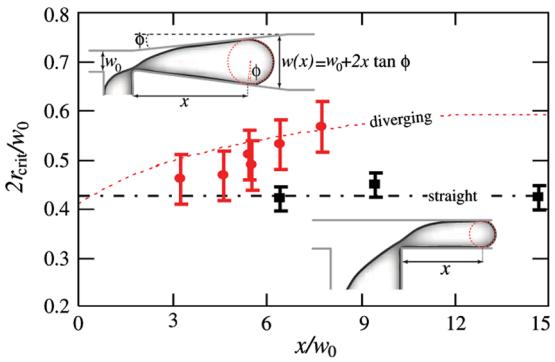

FIG. 5 (color online). Neck radius at the onset of collapse for a bubble that expands downstream of the T junction. Error bars are as in Fig. 4. We varied the liquid feed rate to drive the bubble further into the channel, and we plot the neck radius here versus the distance x/w that the bubble has traveled into the expanding channel at the start of collapse. Diverging channel: $(h, w_0, w_{\mathrm{in}}) = (49, 71, 118)\ \mu$m, $\phi = 7°$, $3\ \mu\mathrm{L/min} < q_L < 16\ \mu\mathrm{L/min}$. Straight channel: $(h, w, w_{\mathrm{in}}) = (75, 100, 300)\ \mu$m, $(q_L, q_G) = (10, 17), (16, 15), (32, 15)\ \mu\mathrm{L/min}$.

vice versa. We have included in Fig. 5 the critical radius at different bubble lengths in a device with straight channels, where both w_{tip} and r_{crit} do not vary with bubble length. It is crucial to include the shape of the entire bubble in the analysis—a mechanism that considers only the necking region, whether stable or not, could never explain these experiments. In this light, it would be interesting to revisit bubble and droplet formation in flow-focusing devices using micrographs of the entire growing droplet.

Up to now, we have focused on the onset of collapse, which depends on the sign of the pressure drop over the gutters rather than the absolute values. We now discuss the velocity in the gutters. An initial estimate would predict that the gutter velocity behaves as $u_{\mathrm{gutter}} \propto a^2 \Delta p / \eta L_{\mathrm{gutter}}$, with as proportionality constant a resistance that depends on the geometry of the gutter. Numerical values for this resistance have been obtained by Wong [12], based on a hydrostatic interface shape in the gutter. We have tried unsuccessfully to find agreement for our experiments with this resistance. Instead we found, invariably, that the experimental velocity was an order of magnitude higher than expected. Equally remarkable, the velocity in the gutters increases with increasing bubble length: Fig. 2(a) shows that initially, the squeezing is adequately described without leakage. In our view, these observations indicate that the interface in the gutter rearranges such that the resistance decreases. Indeed, recent simulations of bubbles in shallow channels [17] show that liquid migrates from the lubricating film on the top and bottom wall to the gutters (resembling the drainage of Plateau borders in foams). This significantly reduces the flow resistance and makes the resistance much less dependent on the aspect ratio h/w. Our observation from dR/dt is that the time-averaged leakage is approximately $0.1 q_L$, independent of h/w. This has important implications beyond bubble generation: the connectivity of pores is a crucial parameter in microscopic models for two-phase flow in porous media [18], relevant in fields such as oil recovery and lung opening. Our finding, that liquid fluxes around ''blocking'' bubbles are much more pronounced when these bubbles move, helps to understand fluid rearrangement in such networks. Top-view images can give the false impression that a bubble blocks a channel, whereas in reality fluid segments are much more interconnected.

We have shown that, in confining geometries, reverse flow around a thread of gas determines when a neck collapses rapidly to release a bubble. This flow, which runs in the direction opposite of the main flow, depends on the curvature of the tip of the thread. As a result, one must consider the confining geometry around the entire thread and not only where the thread will break. This understanding of flows in the gutters is crucial in many flow problems of bubbles and droplets in confined geometries, such as bubble splitting [19]. The challenge is now to use the qualitative understanding of interface rearrangement in the gutters to quantify fluxes around bubbles and droplets during formation, travel, and breakup in microfluidic channel networks and porous media. From a practical point of view, our analysis describes the evolution of the neck in terms of geometric parameters h, w, and w_{in}. Provided the initial condition of the squeezed bubble is known, this allows a prediction of the size of bubbles without empirical constants, a useful extension of the scaling rule for bubble volume [3].

We wish to thank Saif Khan, Rob Mudde, and Axel Guenther for helpful discussions. We thank DC-SIP of Delft University for financial support. M. T. K. is supported by a Veni grant of NWO.

*m.t.kreutzer@tudelft.nl

[1] Lord Rayleigh, Proc. R. Soc. London **29**, 71 (1879); Philos. Mag. **34**, 177 (1892); J. Plateau, *Statique Expérimentale et Théoretique des Liquides Soumis aux Seules Forces Moléculaires* (Gautier-Villars, Paris, 1873).
[2] T. Thorsen *et al.*, Phys. Rev. Lett. **86**, 4163 (2001).
[3] P. Garstecki *et al.*, Lab Chip **6**, 437 (2006).
[4] S. L. Anna, N. Bontoux, and H. A. Stone, Appl. Phys. Lett. **82**, 364 (2003); A. M. Gañán-Calvo and J. M. Gordillo, Phys. Rev. Lett. **87**, 274501 (2001); D. Funfschilling *et al.*, Phys. Rev. E **80**, 015301(R) (2009);
[5] P. Garstecki, M. J. Fuerstman, and G. M. Whitesides, Phys. Rev. Lett. **94**, 234502 (2005).
[6] Various applications are discussed in A. Günther and K. F. Jensen, Lab Chip **6**, 1487 (2006); B. T. Kelly *et al.*, Chem. Commun. (Cambridge) **18**, 1773 (2007).
[7] G. F. Christopher *et al.*, Phys. Rev. E **78**, 036317 (2008).
[8] S. L. Goren, J. Fluid Mech. **12**, 309 (1962); P. S. Hammond, J. Fluid Mech. **137**, 363 (1983); P. Guillot, A. Colin, and A. Ajdari, Phys. Rev. E **78**, 016307 (2008).
[9] B. Dollet *et al.*, Phys. Rev. Lett. **100**, 034504 (2008).
[10] P. Garstecki, H. A. Stone, and G. M. Whitesides, Phys. Rev. Lett. **94**, 164501 (2005).
[11] A. S. Utada *et al.*, Science **308**, 537 (2005).
[12] H. Wong, S. Morris, and C. J. Radke, J. Colloid Interface Sci. **148**, 317 (1992).
[13] H. Wong, C. J. Radke, and S. Morris, J. Fluid Mech. **292**, 95 (1995).
[14] L. L. Shui *et al.*, Appl. Phys. Lett. **93**, 153113 (2008).
[15] V. van Steijn, M. T. Kreutzer, and C. R. Kleijn, Chem. Eng. Sci. **62**, 7505 (2007).
[16] This can be understood from a scaling analysis of the squeezing in Ref. [3]. Estimating that during the filling stage the bubble grows to a volume $\sim w w_{\mathrm{in}} h$ and estimating that the neck squeezes in a time $t_{\mathrm{sq}} \sim h w w_{\mathrm{in}} / q_L$ that allows the bubble to grow by an additional volume $q_G t_{\mathrm{sq}}$, the bubble length scales as $L/w_{\mathrm{in}} \approx 1 + \alpha q_G / q_L$, with geometry-dependent α.
[17] A. De Lozar, A. Juel, and A. L. Hazel, J. Fluid Mech. **614**, 173 (2008).
[18] R. Lenormand, C. Zarcone, and A. Sarr, J. Fluid Mech. **135**, 337 (1983).
[19] A. M. Leshansky and L. M. Pismen, Phys. Fluids **21**, 023303 (2009).
[20] L. Ménétrier-Deremble and P. Tabeling, Phys. Rev. E **74**, 035303(R) (2006).